Satellite Bulk Tropospheric Temperatures as a Metric for Climate Sensitivity

John R. Christy and Richard T. McNider

Earth System Science Center, The University of Alabama in Huntsville, Alabama, USA

Abstract: We identify and remove the main natural perturbations (e.g. volcanic activity, ENSOs) from the global mean lower tropospheric temperatures (T_{LT}) over January 1979 - June 2017 to estimate the underlying, potentially human-forced trend. The unaltered value is +0.155 K dec^{-1} while the adjusted trend is +0.096 K dec^{-1}, related primarily to the removal of volcanic cooling in the early part of the record. This is essentially the same value we determined in 1994 (+0.09 K dec^{-1}, Christy and McNider, 1994) using only 15 years of data. If the warming rate of +0.096 K dec^{-1} represents the net T_{LT} response to increasing greenhouse radiative forcings, this implies that the T_{LT} tropospheric transient climate response (ΔT_{LT} at the time CO_2 doubles) is +1.10 ± 0.26 K which is about half of the average of the IPCC AR5 climate models of 2.31 ± 0.20 K. Assuming that the net remaining unknown internal and external natural forcing over this period is near zero, the mismatch since 1979 between observations and CMIP-5 model values suggests that excessive sensitivity to enhanced radiative forcing in the models can be appreciable. The tropical region is mainly responsible for this discrepancy suggesting processes that are the likely sources of the extra sensitivity are (a) the parameterized hydrology of the deep atmosphere, (b) the parameterized heat-partitioning at the ocean-atmosphere interface and/or (c) unknown natural variations.

Key words: Climate sensitivity, satellite temperatures, volcano, El Niño

1. Introduction

With 15 years (1979-1993) of global lower tropospheric temperature observations (T_{LT}, temperature of the layer from the surface to approximately 300 hPa), we sought, in 1994, to determine the atmosphere's underlying long-term trend by removing the impacts of large natural, interannual fluctuations of that period (Christy and McNider, 1994, hereafter CM94). This was especially important at the time because significant cooling from Mt. Pinatubo's eruption (1991) near the end of the period had tilted the 15-year trend to be negative; −0.04 ± 0.03 K dec^{-1}. By removing these perturbations, a better representation of the basic "long-term" warming rate could be found. Our result in CM94, when the impacts of the El Niño - Southern Oscillation (*ENSO*) events and volcanoes were removed, gave an underlying trend of +0.09 ± 0.03 K dec^{-1}, a

difference of +0.13 K dec^{-1} relative to the actual trend. At the time, a rate of +0.09 K dec^{-1} was less than one-third the rate predicted for warming in climate models due to the enhancement of the greenhouse gas (*GHG*) effect.

Now with a period over two and one-half times longer (38 years, 6 months, Jan 1979 - Jun 2017) of T_{LT} observations, we revisit and improve on CM94. One feature has now changed; rather than volcanic impacts occurring late in the period, they now depress temperatures in the first half, effectively tilting the trend to be more positive than it would otherwise be. There have been some remarkable *ENSO* events as well, e.g. 1997-98 and 2015-16. We shall take CM94 further and calculate an index of climate sensitivity. We focus on the bulk atmospheric layer T_{LT} rather than surface temperature for estimating climate sensitivity as it (a) is more systematically measured both geographically and instrumentally, (b) represents a more climate-relevant quantity of atmospheric heat content, a change in which is a consequence of enhanced *GHG* forcing, (c) represents a large signal due to the negative lapse-rate feedback process in which the trend magnitude (i.e. response) is expected to be greater in the troposphere than the surface, (d) does not suffer from problems affecting surface temperature time series (see below) and (e) has not until now been examined in the context of a climate sensitivity metric. We shall use the previous version of University of Alabama in Huntsville (UAH) T_{LT} (v5.6, Christy et al., 2011) rather than newly updated v6.0 of T_{LT}, (Spencer et al., 2017). We do so to allow these results to be representative of results from global radiosonde and reanalyses datasets whose separate averages generate global trends that are within ± 0.01 K dec^{-1} of UAH v5.6 (Christy, 2017). However, we shall provide and comment on the results from v6.0 in the final discussion. A list of all data sources is given in Table 1.

With a length of 38.5 years, a time series adjusted for these natural perturbations may provide a more robust understanding of temperature changes relative to the weak but gradually increasing *GHG* radiative forcing than detected in surface temperatures whose variations are affected by non-greenhouse issues such as human development. This also allows us to suggest a new metric of climate sensitivity based on tropospheric temperatures for comparison with model simulations. Additionally, a reexamination of the underlying trend is useful now given the relatively flat global tropospheric temperature trend from the *ENSO* of 1997-98 to just prior to the major warm

Corresponding Author: John R. Christy, Earth System Science Center, The University of Alabama in Huntsville, Huntsville, AL, 35899, USA.
E-mail: Christy@nsstc.uah.edu

Table 1. Data sources used in this study.

Name	Type	References
UAH T_{LT} v5.6	Satellite	Christy et al. 2011
UAH T_{LT} v6.0	Satellite	Spencer et al. 2017
RSS T_{LT} v3.3	Satellite	Mears and Wentz 2009
RSS T_{LT} v4.0	Satellite	Mears and Wentz 2017
UVienna	Radiosonde	Average of RAOBCORE and RICH
RAOBCOREv1.5	Radiosonde	Haimberger et al. 2012
RICHv1.5	Radiosonde	Haimberger et al. 2012
NOAA/RATPAC-A2	Radiosonde	Free et al. 2005
UNSW	Radiosonde	Sherwood and Nishant, 2015
CMIP-5 RCP4.5 Model Output	Climate Models	Flato et al. 2013, Output available from van Oldenbrogh 2016

ENSO of 2015-16, which has created a significant divergence between observations and models (McKitrick and Vogelsang, 2014).

Our study will attempt to estimate the basic response of the bulk atmosphere to enhanced greenhouse forcing, i.e. the sensitivity to forcing, as the possible cause for much of the mismatch between observed and modeled temperature trends with a period more than two and one-half times as long as CM94. We recognize that there may be even longer-term internal modes of variability that may be affecting the observed trends. However, in the absence of specific information on such trends [note we have accounted for Atlantic Multi-decadal Oscillation (AMO) and Pacific Decadal Oscillation (PDO)], the present 38.5-year period is our best-observed period to examine model performance and tropospheric sensitivity to increasing radiative forcing. With this study we will test the hypothesis that the climate response of the Intergovernmental Panel on Climate Change (IPCC) Climate Model Intercomparison Project-5 (CMIP-5) models is significantly greater than that calculated from observations.

2. Method and results

In the following we describe the method and calculate the impacts on the global T_{LT} time series of the *ENSO* events and the volcanic events.

a. The ENSO or SST effect

The *ENSO effect* in CM94 was calculated by simple linear regression between the global mean anomaly of T_{LT} and the sea surface temperature anomaly (*SST*) of a region in the central equatorial Pacific Ocean, known as Niño 3.4. Most of the T_{LT} variance was explained when global T_{LT} lagged $SST_{niño3.4}$ by 5 months. Here we shall alter this calculation not by using one *SST* predictor, but the best two of nine *SST* and *SST*-based

predictors.

The first four potential *SST* predictors are the familiar *ENSO SST* monthly anomaly indices from the tropical Pacific Ocean: Niño 1+2, Niño 3, Niño 3.4, and Niño 4. (NOAA sstoi. indices). Added to these four indices will be two tropical Atlantic *SST* indices, N. Atlantic (5°-20°N, 30°-60°W) and So. Atlantic (0°-20°S, 30°W-10°E.) (NOAA sstoi.atl.indices). We also now include three indices that are largely based on regional *SST*s, the Multivariate ENSO Index (*MEI*, Wolter and Timlin, 2011), the Pacific Decadal Oscillation index (PDO, Mantua and Hare, 2002), and the Atlantic Multidecadal Oscillation (AMO, Schlesinger and Ramankutty, 1994).

Because the troposphere tends to lag behind SST changes, i.e. being forced through changes in fluxes of sensible and latent heat, we also tested a time series of tropical Indian Ocean SSTs (IO) as a predictor, but do not include it in the main results below. The IO index explained marginal variance in the southern mid-latitude zones of temperature, but there was no decrease (and in some cases an increase) in the error variance (described later) of the adjusted global temperature time series.

We will also expand the dimension of the predictand or target variable from a single global value used in CM94 to individual 2.5° latitude-bands of T_{LT} anomalies (82.5°S to 82.5°N, 66 in total). Each latitude-band will now require an individual regression equation. Since we have broadened the predictor dataset to include regions outside the Pacific Ocean, this effect will be called the *SST effect* rather than the *ENSO effect*.

With nine potential predictors and lag allowances from 0 to 12 months to predict each latitude-band individually, we also expand the linear regression calculation to include the top two predictor sets (a "set" is one *SST* predictor with its associated lag) rather than just one. With so many opportunities for the variance to be explained by nine sets of *SST* predictors, every latitude-band will have some level of variance explained simply due to chance. After testing a range of parametric options, we determined that the top two sets of predictors would be utilized only if in combination they explain over 25% of the variance for a particular latitude-band's T_{LT} anomalies. Once these are determined latitude by latitude, the global average will then be computed.

One further issue here is the selection of the time period chosen to calibrate the *SST* regression equations. Because the cooling due to the two major volcanoes essentially overpowers the *SST effect* on global temperature, especially Mt. Pinatubo, it was necessary to select a period free from these influences.

We tested numerous periods for calibrating the *SST* co-efficients and lags, examining three quantities of error statistics to decide whether the calibration period was effective. The statistical quantities were, (a) the variance of the 38.5-year adjusted, detrended time series (lower the better), (b) the variance explained by the volcanic impact in the 60 months following the eruption of El Chichon and (c) as in (b) but for Mt. Pinatubo (see below, higher the better). These *SST*

Table 2. Examples of three of the 25 qualifying runs (detrended Var < 0.0140) based upon period over which the calibration of the *SST effect* on global T_{LT} is performed. The mean of the 25 runs is "25 run Mean." The original variance of the monthly T_{LT} time series is +0.0610 K^2 (detrended +0.0350 K^2) and the original global trend is +0.155 K dec^{-1}. "SST Cal" is the calibration period used and "SST Trend" is the linear trend of the global T_{LT} anomalies reconstructed only from the *SST* predictors. The three constants in the volcanic equation are α_0, γ_0 and τ_0. "EC" and "MP" are the variances explained over the 60 months following the eruptions by the volcanic equation for El Chichon and Mt. Pinatubo respectively. "DeTrnd Var" is the variance remaining after the *SST effect, volcanic effect,* and linear trend are removed. "Adj. Trend" is the trend of the residuals after the *SST* and *volcanic effects* have been removed.

SST Cal	*SST* Trend K dec^{-1}	α_0	γ_0	τ_0	EC, MP %	DeTrnd Var K^2	Adj. Trend K dec^{-1}
1995-2004	+0.008	0.19	0.50	21	78, 92	0.0134	+0.100
1997-2005	+0.002	0.19	0.46	24	78, 91	0.0135	+0.105
2009-2017	+0.023	0.25	0.32	26	80, 90	0.0138	+0.085
25 run Mean 95% Range	+0.007 ±0.019	0.22	0.43	24	79, 91	0.0137	+0.096 ±0.012

calibration periods were found to perform best if the period 1997-98 or 2015-16 were included since these *ENSO* events contained considerable variance explainable by the various *SST* indices. We used all periods with beginning dates in July of years 1994 to 1997 and ending dates in June of years 2001 to 2017, for 68 outcomes. To this we added 15 runs that ended in 2017, starting in years 2001 to 2015 giving a total of 83 experiments overall. To focus on the most useful results, we set thresholds for (a) of 0.014 K^2 (i.e. explaining at least 55% of the unadjusted detrended variance), (b) 75% and (c) 90% as minimum requirements for keeping an experiment. These criteria produced 25 runs that qualified.

b. The volcanic effect

In CM94, the *volcanic effect* on the global time series was approximated by a gamma-like function whose magnitude and time constant were related to the square-root of the lower stratospheric temperature perturbation (T_{LS}, also from UAH v5.6 microwave data). The function mimics the time evolution of the impact of the varying concentrations of solar-active aerosols that experience a rapid rise followed by a slow decline. The relative perturbation of the stratosphere is an indicator of the amount of volcanic aerosols injected into the stratosphere and thus the magnitude of their reflective (cooling) potential (Christy and Drouihlet, 1994).

$$T_{LT:vol} = \alpha j^\gamma \, [exp(-j/\tau)] \qquad (1)$$

where $\alpha = \alpha_0 (\Delta T_{LS})^{0.5}$; j is months since eruption; $\gamma = \gamma_0$ and $\tau = \tau_0 (\Delta T_{LS})^{0.5}$.

We shall employ this same formulation with ΔT_{LS} being 0.85 K for El Chichon (Mar 1982) and 1.40 K for Mt. Pinatubo (Jun 1991). The values of α_0 (amplitude of response), τ_0 (time-scale of decay) and γ_0 (non-linear time factor) will be determined by reduction-of-variance which produces a simultaneous best-fit to the two volcanic events after the *SST effect* is removed. (We examined the potential impact of small volcanoes after Mt. Pinatubo, but found no relationship to the small changes in optical depth and the stratospheric temperature).
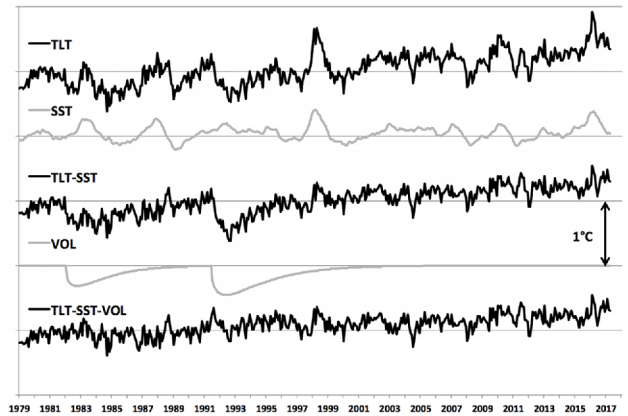

Fig. 1. Time series (1979-2016.5) of global T_{LT} and adjustments applied for the SST calibration period of 1995-2004. The horizontal axes are separated by 1 K. "T_{LT}" is the global average original time series. "SST" is the reconstruction of T_{LT} based on the *SST* predictors. "T_{LT} - SST" are the residuals of T_{LT} after subtracting the *SST* dependence. "VOL" is the cooling effect calculated from the volcano equations. The bottom time series is the T_{LT} residual after the *SST* and *VOL* effects are removed.

c. Results

The results in Table 2 show examples of three individual experiments and the overall average of the 25 runs that qualified according to the criteria set out in section 2a. Figure 1 displays the time series as the steps were applied to an example experiment in which the *SST* calibration period was 1995-2004. The results (25 runs) indicate that the underlying median adjusted trend is +0.096 ± 0.012 K dec^{-1} for the UAH T_{LT} time series. This is essentially the same value we determined in CM94 where less sophisticated techniques were applied over a period less than half the length. We draw two points from the evidence in Table 2, (1) the time series is of sufficient length that the trend-impact of the *SST effect* is near zero (i.e. not significantly different from zero) and thus the *volcanic effect* dominates, and (2) removing the impact of the two volcanoes imposes a less positive tilt on the global T_{LT} trend being about 62 percent of the original (+0.096 vs.

+0.155 C dec^{-1}). It should be noted that the residual T_{LT} here is almost identical to the recent residual trend of a later independent study using slightly different assumptions on *SST* regions and volcanic contributions and such independent replications are important in science (Santer et al., 2014).

An examination of Total Solar Irradiance (*TSI*) was undertaken to determine if a clear relationship was discoverable. The amplitude of the 11-year cycle has diminished since the peak in 2000 and, in our residual time series, there is indeed a slight slowdown in the rise after 1998. One may arbitrarily select an accumulation period of *TSI*, so that a peak occurs near 1998 so the *TSI* coincides with (explains) variations in T_{LT} (e.g., a 22-year *TSI* trailing average peaks in 2000, though other averaging periods do not), but this would compromise the independence between the predictors and predictand. We do not suggest that solar variations cannot influence global T_{LT}, and other studies offer evidence in support (e.g. Scafetta, 2013), but our view here is that if there is a small 10-20 year influence, the length of our time series (38.5 years) will include at least a full cycle with a peak near the center of the period, so that its trend will not seriously be affected.

3. Tropospheric Transient Climate Response (*TTCR*)

a. Estimate of TTCR from observations

To address climate sensitivity we first assume that T_{LT} basically represents a heat content reservoir with a relatively fast temperature response to forcing. This reservoir integrates all of the components that influence the accumulation or depletion of energy from variable forcing introduced from, for example, (a) solar anomalies (including volcanic shading), (b) variations of non-radiative energy input (e.g., latent heat release), (c) ocean temperature fluctuations (which themselves are caused by circulation and/or cloud extent variations among other causes) and (d) enhanced *GHG* and other anthropogenic forcing. Again, our view is that T_{LT} is an important quantity to study in terms of sensitivity because of the bulk mass that it represents in terms of climate response, though the ocean is by far the largest reservoir of heat content. The volcanic events are independent of human forcing and given that the trend of the tropical ocean (i.e., *SST*) "forcing" is virtually zero, we are assuming this too is independent of human activity over this time period.

The climate system contains within itself many degrees of freedom and thus possess the capability to create variations over decades due to natural, unforced internal dynamical processes which then may be manifested in, for example, 38.5-year linear trends. However, here we shall assume that the net impact of this decadal scale natural variability has been near zero since 1979 and that the underlying trend due to the net impact of human influences is +0.096 ± 0.012 K dec^{-1}, where the error range represents the spread of the various simulations. We are not defending this rather bold assumption regarding natural variability, but simply stating it as a basis for going forward to derive climate sensitivity estimates, acknowledging the strong dependence on this assumption to what follows.

One measure of sensitivity is the Transient Climate Response (*TCR*), defined as the surface temperature achieved at the time of doubling of CO_2 when increased at a rate of 1 percent per year compounded (reached at year 70 in the integration, Collins et al., 2013). *TCR* is a "more informative indicator of future climate" than the equilibrium climate sensitivity because the real world also experiences *GHG* forcing as a gradual increase (Collins et al., 2013). As noted above, we shall use T_{LT}, rather than surface temperature, and define our metric as Tropospheric *TCR* (*TTCR*) from observations is expressed by:

$$TTCR = F_{2x} \Delta T_{LT} / \Delta F \qquad (2)$$

where $F_{2x} = 3.7$ Wm^{-2}, ΔT_{LT} is the measured T_{LT} change over a period in which the change in F (ΔF) occurs. This equation seems reasonable as the temperature response in climate models to steadily increasing radiative forcing is essentially linear. *TTCR* has some advantages over *TCR* in that the temperature observations (T_{LT}) represent a bulk layer of the atmosphere as opposed to the surface temperature in *TCR* which can be strongly influenced by land use changes, sensitivity to nighttime temperatures and uncertainties in ocean surface temperatures (Pielke Sr. et al., 2007; Christy et al., 2009, 2010; McNider et al., 2012) Additionally, T_{LT} has uniform global coverage which is consistent with the forcings used in defining *TTCR*.

Applying the definition of *TTCR* to our adjusted trend of +0.096 K dec^{-1}, we have $\Delta T_{LT} = +0.368$ K over a period in which the increase in *GHG* forcing (CO_2, tropospheric O3 and other well-mixed *GHG*s) was estimated as 1.45 Wm^{-2} (Myhre et al., 2013). The total ΔF which includes other human influences (tropospheric aerosols, land-use change, etc.) was estimated to have increased by 1.24 Wm^{-2} (Myhre et al., 2013). Thus, if our adjusted warming of +0.368 K represents the response to a total anthropogenic ΔF of +1.24 Wm^{-2} then the response to *GHG* alone for the period should be +(1.45)(0.368)/(1.24)K or +0.430 K in total giving a trend of +0.112 K dec^{-1}. Applying these values to calculate *TTCR* we have (3.7)(0.430)/(1.45) K = 1.10 K as the central value of the observational calculation. As a side note, it is a coincidence that the doubling of GHG forcing is anticipated to occur about 100 years from 1979, so that the *TTCR* value will be very near the century-scale trend value of the adjusted T_{LT} data calculated for 1979-2016.5. Applying error estimates of the adjustments to temperature time series (± 0.012 K dec^{-1}) and of the observational error itself (± 0.030 K dec^{-1}, which accommodates all other observational trend magnitudes noted later) we calculate a value of *TTCR* as 1.10 ± 0.26 K.

One potential error in the *growth* of the forcing terms could be in the aerosol term which is included in the total change in forcing (1.24 Wm^{-2}) as errors in *GHG*-only forcing will affect both the total and *GHG*-only in the same way. However, the absolute magnitude of the aerosol forcing term was estimated

to change only slightly in these 38.5 years (-0.15 Wm^{-2}), so we may assume errors in the *growth* of the forcing would be even smaller (Myhre et al., 2013). Indeed recent research suggests the aerosol forcing may be less negative than assumed, which in turn would lower the *TTCR* calculated here (Bianchi et al., 2016). [Note: errors in the forcing values will impact the calculated *TTCR* here and the model values below in the same way and thus will not affect the conclusions of the comparison study performed below.]

b. Estimates of TTCR from model simulations

An estimation of *TTCR* from the average model may be calculated in a number of ways and we shall look at three different methods. We shall concentrate only on the average of the model runs since we have a large sample ($N = 102$) and thus high confidence in what the mean of the model population is. In other words, there is essentially no "error" in knowing what the *average* is. Also, by averaging 102 model runs, we will have effectively eliminated the impact of ENSO events and other short-term climate variability on the resulting time series, while any average greenhouse gas influence will remain. We will not judge the models as to which might be more realistic than others, but simply demonstrate the outcome of this analysis of their *average* and thus our conclusions will apply only to the *average* of the CMIP-5 using the "reference concentration pathway" which peaks at a forcing of 4.5 (RCP4.5) models, not to the spread. We note that there is no material difference between RCP4.5, 6.0 and 8.5 through about 2030. For informational purposes the 95 percent confidence interval will be given in various places.

First, the IPCC provides *TCR* for surface temperature for the models utilized in this study and which averages 1.8 ($\pm$ 0.6) K (Flato et al., 2013). Using all 102 Climate Model Intercomparison Project-5 (CMIP-5) global models (KNMI Climate Explorer, van Oldenbrogh, 2016), we calculated the rate of global T_{LT} warming relative to the surface temperature trend and found an average amplification factor in the models of 1.18 ($\pm$ 0.13). This indicates an estimate of the *TTCR* of the *average* CMIP-5 model is 2.12 K (i.e. *TTCR* = (1.18) (1.8)).

Secondly, we may calculate the model-average warming rate during this period from a portion of the time series that was not affected by volcanic activity (Fig. 2). This is possible because with a sample size of 102 members (averaged into 25 groups), portions of the time series are still relatively smooth. If we select 2001-2016 (beginning 10 years after the eruption of Mt. Pinatubo), the model average trend is +0.252 K dec^{-1}, i.e. less than the actual 1979-2016 model-average trend of +0.273 K dec^{-1}. Assuming this would be the trend over the entire time series over which the stated anthropogenic forcing values are available, we calculate, as was done with the observations with estimated 38.5-year GHG forcing of 1.45 Wm^{-2}, that *TTCR* is 2.48 K.

Thirdly, we are able to estimate the *TTCR* from simulations using the RCP4.5 scenario over a period of linear *GHG* anthro-
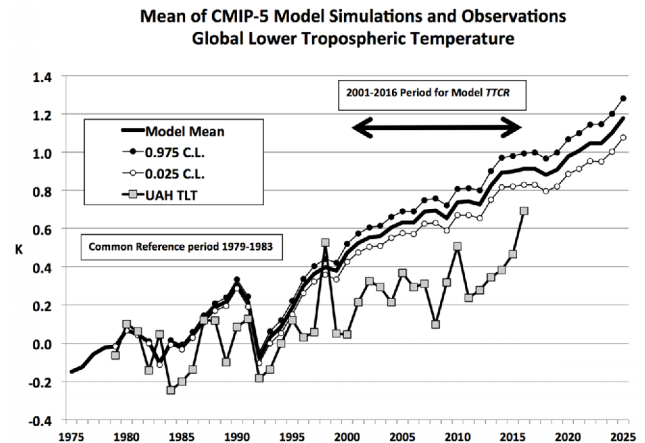

Fig. 2. Time series of the average of the 25 model groups (thick line) using 102 individual simulations of T_{LT} from 1975-2025 (RCP45, see text). The spread of the time series is calculated by determining the standard error of the mean trend of the individual time series for the 97.5 and 2.5 percent confidence limits. The time series of the observed T_{LT} from UAH v5.6 is also shown. All times series are referenced to the period 1979-1983.

pogenic forcing in the scenario prescription, 2001-2050. T_{LT} of the 102 CMIP-5 models warmed 1.26 K on average over this period when the *GHG* ΔF for RCP4.5 was prescribed as 2.0 Wm^{-2} (Collins et al., 2013). This yields an estimate of *TTCR* as (3.7)(1.26)/(2.0) K = 2.33 K (ΔF was due essentially to an increase in well-mixed greenhouse gases only). This is likely the best estimate as it uses the longest time period, the defined metric of T_{LT}, and is responding to prescribed forcing.

Using these three separate calculations, the value of the average CMIP-5 model's *TTCR* is calculated to be 2.31 $\pm$ 0.20 K or double that calculated from direct observations. This suggests that the fundamental issue in explaining the mismatch between 38.5 years (not merely the recent 18-year hiatus) of observed climate warming versus modeled warming may be that models are too sensitive to enhanced radiative forcing. The study of Santer et al. 2014, while using nearly the same observed T_{LT} as here and the same CMIP-5 model trends, suggested that better agreement between models and observed T_{LT} in the early part of the record in response to the volcanic impacts means there is not a systematic error in the models in the handling of anthropogenic greenhouse warming (AGW). However, due to the volcanic forcing this was a period of either cooling or little change in the actual and modeled T_{LT} thus there is no clear opportunity to test in this period the positive water vapor or cloud feedbacks that amplify the AGW over longer periods. The sensitivity here in which the entire length of record is utilized suggests, over all, greater sensitivity in the models.

The more recent version 6.0 of UAH T_{LT}, which has a considerably different construction process from v5.6, generates a 1979-2016.5 global trend of +0.124 K dec^{-1}, an adjusted trend of +0.074 K dec^{-1}, and a calculated *TTCR* of +0.84 K. Similarly, scaling global trends from other producers of T_{LT} as
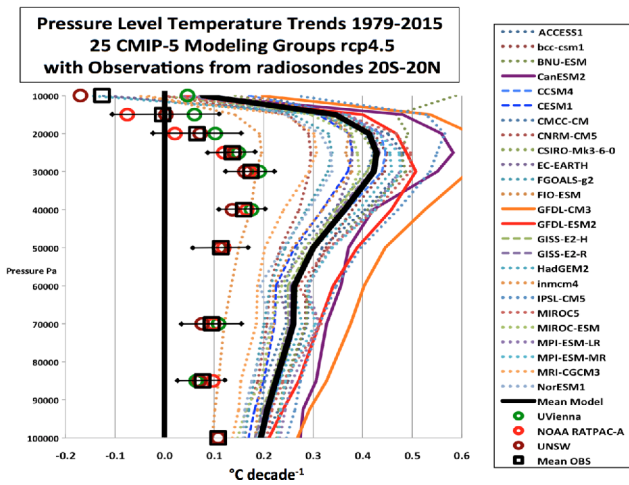
Fig. 3. Pressure-level temperature trends (1979-2016) for the tropical atmosphere as measured by four radiosonde datasets (circles with square as average, UVienna is average of two datasets) and 25 modeling groups (dotted, dashed and solid lines, mean is black line) used in the IPCC AR5.

published in Christy (2017), we have a range of *TTCR* values from +0.93 to +1.30 K (highest from Remote Sensing Systems v4.0, Mears and Wentz, 2017). These values are accommodated in our main result calculated earlier; 1.10 ± 0.26 K. Another point to mention is that if the aerosol cooling term is too large and then is reduced, this would imply that less warming is accounted for by the *GHG* forcing term. These additional evidences indicate the *TTCR* calculated above as 1.10 K, could be even less. Thus, our results support the hypothesis that the observed *TTCR* is half (or less) than that of the CMIP-5 models on which projections of the future climate are based.

c. Discussion of observational and model differences in TTCR

Differences between empirical and modeled surface-defined values of *TCR* and equilibrium climate sensitivity (*ECS*) were noted in the IPCC (Collins et al., 2013). They indicated that model-calculated *ECS* was on average greater than empirically-calculated values, summarized in IPCC, while closer agreement was found relative to *TCR* (Collins et al., 2013). Our results, however, indicate a greater discrepancy using the *TTCR* metric than shown in the IPCC because the negative lapse rate feedback generates a greater response throughout the troposphere in models than at the surface (National Academy of Sciences, 2003). Thus, discrepancies are larger using the troposphere since the evidence indicates the observed atmosphere does not respond with as strong a negative lapse rate feedback as seen in models.

As noted, the *TTCR* of our empirical study is half or less than that in the CMIP-5 model average. We believe that the fact the larger discrepancies appear in the troposphere likely points to the reasons for the difference. Additionally, the region of the largest differences is the tropics. In Fig. 3 we show the comparison of vertical temperature trends for four

observational radiosonde datasets (UVienna is the average of two, see Table 1) and that of the CMIP-5 models as grouped by institutional runs. In every case, with the exception of the Russian model "inmcm4" below 250hPa, individual tropospheric model trends are larger than the observational average below 100 hPa with the discrepancies largest in the upper troposphere (see also Jiang et al. 2012 regarding upper tropospheric humidity where model errors were also largest there). Note that this is true even though the observational results have the added boost of a major warm *ENSO* at the end of their time series. [A somewhat more obscure depiction of this same result is found in the IPCC AR5 Supplementary Material in which the observed tropical tropospheric trends are wholly contained within the "unforced" model trends and wholly outside of the "forced with anthropogenic *GHG*" model trends (Fig. 10.SM.1, Bindoff et al., 2013).]

The net tropospheric response to forcing from human impacts is complicated and contains uncertainty (e.g. Spencer and Braswell, 2010; Lindzen and Choi, 2011; Choi et al., 2014). The magnitude of the direct effect of the thermal *GHG* radiative forcing is considered to be fairly well-known while that of anthropogenic aerosols and cloud feedbacks, for example, are not (Forster et al., 2007). However, if our fundamental assumptions are basically correct, then our result suggests the average model response of the atmosphere to this forcing is overdone. Possible reasons for this result are numerous, for example: (1) the growth in the cooling effect of anthropogenic aerosols or other human impacts is understated in models (though IPCC AR5 indicates otherwise, Stocker et al., 2013), (2) the direct warming effect of *GHG* is overstated in models, (3) our assumption that the observations do not contain a significant natural, unforced decadal cooling is incorrect and not captured by any model (see Meehl et al. 2013 for explanations of the possibility), and/or (4) the positive (negative) feedbacks are overstated (understated) in the models. Hope et al. (2017) note that models "tend to warm [the surface] too quickly, on average by about a factor of two", and hypothesize that the climate model feedbacks amplify the radiative forcing due to *GHG* "too strongly". Two such feedback processes are mentioned next.

Because the discrepancy is greatest in the tropical atmosphere, this provides clues as to its cause and we shall suggest two possibilities apart from unknown natural variations mentioned earlier. First, the excessive model warmth in the upper troposphere is related to latent heat released from convective precipitating systems and the subsequent rate of emission of that heat to space in the descending regions. In terms of traditional calculations of climate sensitivity this transfer of heat and moisture to higher levels in the model atmosphere means that the equilibrium radiative temperature of the Earth system will be at a higher elevation. This is because radiation emitted by water vapor or liquid water at the lower temperatures of these higher altitudes would decrease outgoing radiation which in turn would require the Earth's temperature to increase more to come to radiative equilibrium.

It is possible that with warming, the convective systems precipitate more efficiently than in models, thus expelling incrementally drier air to the descending regions where thermal emission to space would be incrementally more efficient, Su et al. (2017) and Choi et al. (2014). This could act to prevent a larger accumulation of heat in the upper atmosphere than seen in models.

Secondly, the heat transfer at the atmosphere-ocean interface is extremely complex and in which the roles of winds, currents, sea state, etc., in models are highly parameterized. Any additional heat transferred to the oceans than is now accounted for in models is a negative atmospheric feedback at least on shorter time scales. It is also possible that a portion of the extra downwelling *GHG* radiative energy rather than going into the atmosphere at the rate, as now modeled, may be remaining on the skin surface and expelled more readily to space through the thermal window, or more rapidly mixed to ocean depths than is now parameterized. In this case, the extra heat never takes up residence in the atmospheric column. Certainly other processes can be operating which explain the lack of heat accumulation in the atmosphere, but these are two leading hypotheses in our view that need further analysis. It is clear, however, that the tropical atmosphere has warmed at a significantly different rate than the average of the CMIP-5 models over the past 38.5 years.

4. Conclusions

The current tropospheric temperature trend from 1979-2016 is influenced by large, natural, interannual fluctuations which if removed reveal a trend about a third less positive than is directly measured (+0.155 down to +0.095 K dec^{-1}). This underlying trend is essentially the same as calculated in CM94 (+0.09 K dec^{-1}) when only 15 years were available and who determined the underlying trend at that time needed adjustment upward, from −0.04 to +0.09 K dec^{-1}. We find that the influence of the tropical oceans and mid-latitude *SST* indices on the temperature trend has been essentially zero since 1979, so that removing the cooling in the early part of the record from the eruptions of El Chichon and Mt. Pinatubo dominates the adjustment.

The assessment of tropospheric climate sensitivity from the calculation of the underlying trend above requires significant assumptions. If we assume, among other things, that the impact of the net of natural external and internal forcing variations has not influenced the observed trend and that anthropogenic forcing as depicted in the average of the IPCC AR5 models is similar to that experienced by the Earth, then observations suggest the tropospheric transient climate response (*TTCR*) is 1.10 ± 0.26 K. This central estimate is likely less than half that of the average of the 102 simulations of the CMIP-5 RCP4.5 model runs also examined here (2.31 ± 0.20). If this result is borne out, it suggests many explanations including the possibility that that the average feedbacks of the CMIP-5 generation of climate models are likely skewed to

favor positive over negative relative to what is present in the actual Earth system. As noted, we cannot totally discount that natural variability or errors in forcing might also account for the discrepancy between modeled and observed *TTCR*. However, given the facts that the processes controlling the uptake of energy by oceans and the transfer of heat in the tropical atmosphere are largely parameterized, it is not scientifically justified to dismiss model error, possibly substantial, as one source of the discrepancy.

Edited by: Kyong-Hwan Seo

References

Bianchi, F., and Coauthors, 2016: New particle formation in the free troposphere: A question of chemistry and timing. *Science*, **2016**, doi: 10.1126/Science.aad5456.

Bindoff, N. L., and Coauthors, 2013: Detection and attribution of climate change: From global to regional. In *Climate Change 2013: The Physical Science Basis.* T. F. Stocker et al. Eds., Cambridge University Press, 867-952.

Choi, Y.-S., H. Cho, C.-H. Ho, R. S. Lindzen, S. K. Park, and W. Yu, 2014: Influence of non-feedback variations of radiation on the determination of climate feedback. *Theor. Appl. Climatol.*, **115**, 355-364, doi:10.1007/s00704-013-0998-6.

Christy, J. R., 2017: Lower and mid-tropospheric temperature. [in State of the Climate 2016]. *Bull. Amer. Meteor. Soc.*, **98**, 16, doi:10.1175/2017BAMSStateoftheClimate.1.

_____, and S. Drouilhet, 1994: Variability in daily, zonal mean lower-stratospheric temperatures. *J. Climate*, **7**, 106-120.

_____, and R. T. McNider, 1994: Satellite greenhouse signal. *Nature*, **367**, 325.

_____, W. B. Norris, and R. T. McNider, 2009: Surface temperature variations in East Africa and possible causes. *J. Climate*, **22**, 3342-3356, doi:10.1175/2008JCLI2726.1.

_____, B. Hermon, R. Pielke Sr., P. Klotzbach, R. T. McNider, J. J. Hnilo, R. W. Spencer, T. Chase, and D. Douglass, 2010: What do observational datasets say about modeled tropospheric temperature trends since 1979? *Remote Sens.*, **2**, 2148-2169, doi:10.3390/rs2092148.

_____, R. W. Spencer, and W. B. Norris, 2011: The role of remote sensing in monitoring global bulk tropospheric temperatures. *Int. J. Remote Sens.*, **32**, 671-685, doi:10.1080/01431161.2010.517803.

Collins, M., and Coauthors, 2013: Long term climate change: Projections, commitments and irreversibility. In *Climate Change 2013: The Physical Science Basis.* T. F. Stocker et al. Eds., Cambridge University Press, 1029-1136.

Flato, G., and Coauthors, 2013: Evaluation of climate models. In *Climate Change 2013: The Physical Science Basis.* T. F. Stocker et al. Eds., Cambridge University Press, 741-866.

Forster, P., and Coauthors, 2007: Changes in atmospheric constituents and radiative forcing. In *Climate Change 2007: The Physical Science Basis.* S. Solomon et al. Eds., Cambridge University Press, 130-234.

Free, M., D. J. Seidel, J. K. Angell, J. Lanzante, I. Durre, and T. C. Peterson, 2005: Radiosonde atmospheric temperature products for assessing climate (RATPAC): A new data set of large-area anomaly time series. *J. Geophys. Res.*, **110**, D22101, doi:10.1029/2005JD006169.

Haimberger, L., C. Tavolato, and S. Sperka, 2012: Homogenization of the

global radiosonde temperature dataset through combined comparison with reanalysis background series and neighboring stations. *J. Climate*, **25**, 8108-8131, doi:10.1175/jcli-d-11-00668.1.

Hope, A. P., T. P. Canty, R. J. Salawitch, W. R. Tribett, and B. F. Bennett, 2017: Forecasting global warming. In *Paris Climate Agreement: Beacon of Hope*. R. J. Salawitch et al. Eds., Springer Climate, 51-113, doi:10.1007/978-3-319-46939-3_2.

Jiang, J. H., and Coauthors, 2012: Evaluations of cloud and water vapor simulations in CMIP5 climate models using NASA "A-Train" satellite observations. *J. Geophys. Res.*, **117**, D1410, doi:10.1029/2011JD017237.

Lindzen, R. S., and Y.-S. Choi, 2011: On the observational determination of climate sensitivity and its implications. *Asia-Pac. J. Atmos. Sci.*, **47**, 377-390, doi:10.1007/s13143-011-0023-x.

Mantua, N. J., and S. R. Hare, 2002: The Pacific decadal oscillation. *J. Oceanography*, **58**, 35-44, doi:10.1023/A:1015820616384.

McKitrick, R. R., and T. J. Vogelsang, 2014: HAC robust trend comparisons among climate series with possible level shifts. *Environmetrics*, **25**, 528-547, doi:10.1002/env.2294.

McNider, R. T., G. J. Steeneveld, A. A. M. Holtslag, R. A. Pielke Sr., S. Mackaro, A. Pour-Biazar, J. Walters, U. Nair, and J. Christy, 2012: Response and sensitivity of the nocturnal boundary layer over land to added longwave radiative forcing. *J. Geophys. Res*., **117**, doi10.1029/2012JD017578.

Mears, C. A., and F. J. Wentz, 2009: Construction of the Remote Sensing Systems V3.2 atmospheric temperature records from the MSU and AMSU microwave sounders. *J. Atmos. Oceanic Technol.*, **26**, 1040-1056, doi:10.1175/2008JTECHA1176.1.

_____, and _____, 2017: A satellite-derived lower tropospheric atmospheric temperature dataset using an optimized adjustment fro diurnal effects. *J. Climate*, **30**, 7695-7718, doi:10.1175/JCLI-D-16-0768.1.

Meehl, G. A., A. Hu, J. M. Arblaster, J. Fasullo, and K. E. Trenberth, 2013: Externally forced and internally generated decadal climate variability associated with interdecadal Pacific Oscillation. *J. Climate,* **26**, 7298-7310, doi:10.1175/JCLI-D-12-00548.1.

Myhre, G., and Coauthors, 2013: Anthropogenic and natural radiative forcing. In *Climate Change 2013: The Physical Science Basis*. T. F. Stocker et al. Eds., Cambridge University Press, 659-740.

National Academy of Sciences, 2003: Cloud, water vapor, and lapse rate feedbacks. In *Understanding Climate Change Feedbacks*. National

Research Council Ed., The National Academy Press, 166 pp.

NOAA, 2017 cited: sstoi.indices. [Available online at http://www.cpc.ncep.noaa.gov/data/indices/sstoi.indices.]

NOAA, 2017 cited: sstoi.atl.indices. [Available online at http://www.cpc.ncep.noaa.gov/data/indices/sstoi.atl.indices.]

Pielke Sr., R. A., and Coauthors, 2007: Unresolved issues with the assessment of multidecadal global land surface temperature trends. *J. Geophys. Res.*, **112**, doi:10.1029/2006JD008229.

Santer, B. D., and Coauthors, 2014: Volcanic contribution to decadal changes in tropospheric temperature. *Nat. Geosci.*, **7**, 185-189, doi:10.1038/ngeo2098.

Scafetta, N., 2013: Discussion on climate oscillations: CMIP5 general circulation models versus a semi-empirical harmonic model based on astronomical cycles. *Earth Sci. Rev.,* **126**, 321-357, doi:10.1016/j.earscirev.2013.08.008.

Schlesinger, M. E., and N. Ramankutty, 1994: An oscillation in the global climate system of period 65-70 years. *Nature,* **367**, 723-726, doi:10.1038/367723a0.

Sherwood, S. C., and N. Nishant, 2015: Atmospheric changes through 2012 as shown by iteratively homogenized radiosonde temperature and wind data (IUKv2). *Environ. Res. Lett.*, **10**, 054007, doi:10.1088/1748-9326/10/5/054007.

Spencer, R. W., and W. D. Braswell, 2010: On the diagnosis of radiative feedback in the presence of unknown radiative forcing. *J. Geophys. Res.*, **115**, D16109, doi:10.1029/2009JD013371.

_____, J. R. Christy, and W. D. Braswell, 2017: UAH Version 6 global satellite temperature products: Methodology and results. *Asia-Pac. J. Atmos. Sci.*, **53**, 121-130, doi:10.1007/s13143-017-0010-y.

Stocker, T. F., and Coauthors, 2013: Technical Summary. In *Climate Change 2013: The Physical Science Basis*. T. F. Stocker et al. Eds., Cambridge University Press, 33-115.

Su, H., and Coauthors, 2017: Tightening of tropical ascent and high clouds key to precipitation change in a warmer climate. *Nat. Commun.*, **8**, 15771, doi:10.1038/ncomms15771.

van Oldenbrogh, G. J., 2016: Climate Data Explorer. [Available online at http://climexp.knmi.nl/selectfield_co2.cgi?someone@somewhere.]

Wolter, K., and M. S. Timlin, 2011: El Niño/Southern Oscillation behaviour since 1871 as diagnosed in the extended multivariate ENSO index. *Intl. J. Climatol.*, **31**, 1074-1087, doi:10.1002/joc.2336.